Computers and Mathematics with Applications 64 (2012) 1226–1234

Contents lists available at SciVerse ScienceDirect

Computers and Mathematics with Applications

journal homepage: www.elsevier.com/locate/camwa

Control of a 3D piezo-actuating table by using an adaptive sliding-mode controller for a drilling process

Hung-Yi Chen *, Jin-Wei Liang

Department of Mechanical Engineering, Ming Chi University of Technology, New Taipei city, 243, Taiwan

ARTICLE INFO

Keywords:
3D piezo-actuating system
Hysteresis nonlinearity
Functional approximation technique
Drilling process

ABSTRACT

Recently, the micropositioner has become an important developing target for achieving the requirements of precision machinery. The piezo-actuating device plays a very important role in this application area. In this paper, a model-free adaptive sliding-mode controller is proposed for a 3D piezo-actuating system because of the system's hysteresis nonlinearity and time-varying characteristics. This control strategy employs the functional approximation technique to establish the unknown function for releasing the model based requirements of the sliding-mode control. The update laws for the coefficients of the Fourier series function parameters are derived from a Lyapunov function to guarantee the control system stability. To verify the effectiveness of the proposed controller, drilling process control using the designed controller is investigated in this paper.

1. Introduction

In recent years, 3D micropositioning technology has become an important developing target for achieving high-resolution requirements of the precision industry, such as in microscopy applications, semiconductor manufacturing processes and opto-electronics systems. Since the piezoelectric actuator has many advantages, such as high resolution, ultrahigh precision and quick response speed, it has been widely used as a micropositioning system actuator in these production areas. However, piezoelectric actuators are ferroelectric and exhibit undesired hysteretic behaviors which lead to inaccuracy problems and limit the tracking performance of the piezoelectric actuated system.

Recently, different methods have been proposed for controlling the piezoelectrically actuated micropositioning system. Lin and Yang [1] employed a PI feedback control associated with feedforward compensation based on the hysteresis observer to compensate the nonlinearity of the piezoelectric actuator. Chang and Sun [2] tried to control a two-degree-of-freedom monolithic piezoelectric actuator. Bashash and Jalili [3] proposed a modeling and control methodology for real-time compensation of nonlinearities along with precision trajectory control of piezoelectric actuators in various ranges of frequency operation. Liaw et al. [4] presented a robust motion tracking control methodology for a flexure based four-bar micro/nanomanipulator driven by a piezoelectric actuator. In addition, control techniques involving feedback and feedforward–feedback features have been proposed to remove the hysteresis-caused tracking error [5]. Meurer and Kugi [6] designed an asymptotically stabilizing tracking controller for an undamped wave equation modeling a piezoelectric stack actuator. Lin and Lin [7] proposed a novel feedforward compensation mechanism based on the Duhem model with crossover terms for obtaining the cross-coupling effects between the X axis and Y axis of a biaxial piezo-actuated positioning stage. For 3D precision positioning applications, Chang et al. [8] presented an ultraprecision three-dimensional micropositioner using a built-in multilayer piezoelectric actuator. The micropositioner was controlled to achieve the goal of nanometer resolution.

* Corresponding author.
E-mail address: hychen@mail.mcut.edu.tw (H.-Y. Chen).

0898-1221/$ – see front matter © 2012 Elsevier Ltd. All rights reserved.
doi:10.1016/j.camwa.2012.03.066

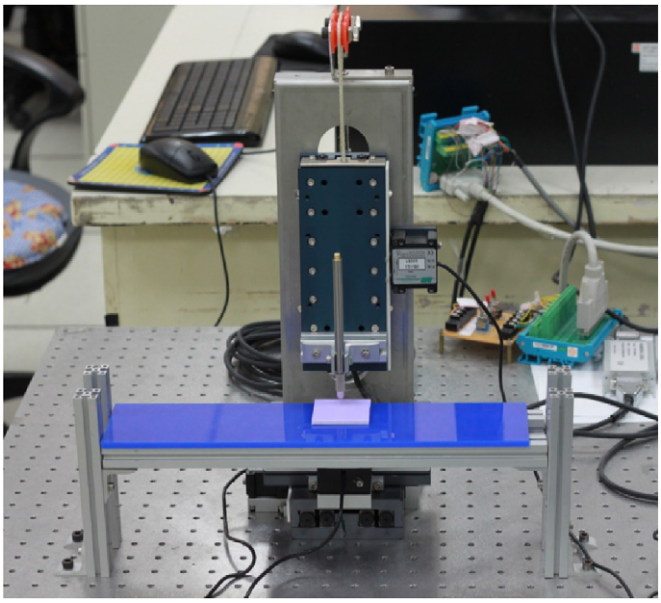

Fig. 1. 3D piezoelectrically actuated drilling system.

Fung and Lin [9] proposed an adaptive backstepping control method for the contour tracking of a plane-type 3D precision positioning table.

It is well known that sliding-mode control can be used to handle system nonlinear behavior, model uncertainty and external disturbance [10–12]. However, the traditional sliding-mode control scheme has model based requirements: it still needs the system dynamic model and the value of the uncertain bound for controller design. Hence, the functional approximation (F.A.) technique is employed to release these model based requirements. The functional approximation technique was utilized to design an adaptive sliding controller for different nonlinear systems containing time-varying uncertainties [13].

In this paper, a functional approximation based adaptive sliding controller is developed for controlling a 3D piezoelectrically actuated system. It has the advantage of designing a sliding-mode controller for a nonlinear 3D piezoelectrically actuated system without the dynamic model requirements. The system uncertainties and the internal states are lumped into a time-varying function with unknown bounds; then, the functional approximation technique is utilized to expand and capture the system dynamics plus uncertainties using finite linear combinations of basis functions with unknown constant weighting vectors. The update laws for the weighting vector of the approximation functions can be derived and the stability of the designed controller is proven in the sense of the Lyapunov stability theorem. Finally, a drilling process control using the designed controller is investigated to verify the effectiveness of the proposed controller.

2. The system structure

A 3D piezoelectrically actuated drilling system shown in Fig. 1 was built for investigating the dynamic system control behavior. A PC based controller is developed for this system. The 3D piezoelectrically actuated drilling system has three independent axes, X, Y and Z, separately driven by three piezoelectric actuators. The experimental layout of this positioning system is shown in Fig. 2 in which the control voltage is calculated on the PC, converted from a digital to an analogue signal by a D/A interface card and sent to the piezoelectric actuator driver unit to actuate the piezoelectric motor for each axis. The displacements of this 3D piezoelectrically actuated system are measured by linear encoders and sent back to the PC via an encoder card for closed-loop control. Three HR8 motors were used to actuate the X, Y and Z axes, respectively. On the basis of the features of these motors, there is a linear relationship between the piezoelectric actuator velocity and the driver control voltage. Therefore, the actuator and driver can be modeled as a DC motor with internal friction. The motor is driven by a voltage amplifier. The driver generates a 39.6 kHz sinusoidal wave to drive the actuator with an amplitude function when a command voltage within ± 10 V is sent to the driver unit. This constant oscillation frequency is generated from the driver unit which was supplied by Nanomotion Limited.

In addition to the nonlinear hysteresis, a dead-zone offset voltage can also be observed in the X–Y–Z table system. Such a nonlinearity appearing in the low control voltage range is called the dead-zone offset voltage because it is caused by the static friction and preload. The dead-zone offset voltage is time-varying. Therefore, its value changes with the operation time,

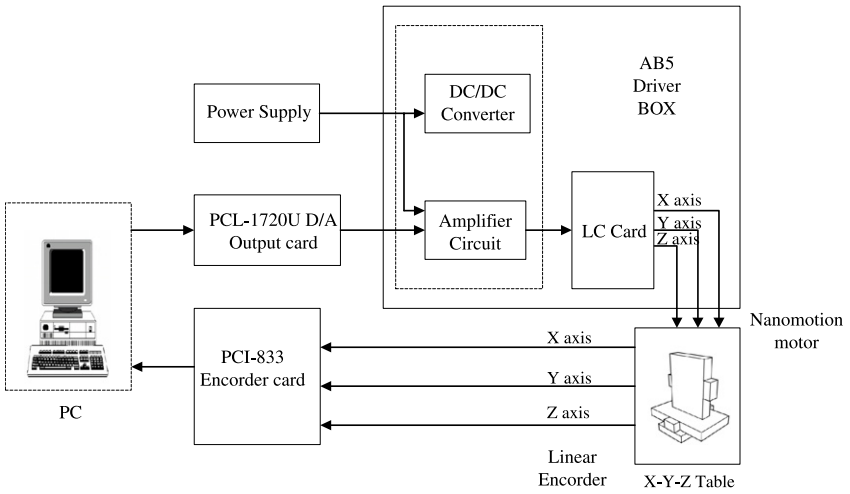

Fig. 2. System experimental layout.

direction, humidity and temperature. In order to handle the complexity of the system's behaviors, the nonlinearities, such as the hysteresis and dead-zone offset, and the time-varying uncertainties will be lumped into an unknown time-varying function. Then, the functional approximation based adaptive sliding-mode control scheme is applied to approximate this time-varying function.

To simplify the model description, the system dynamics for each of the three axes can be represented using the following second-order model:

$$\ddot{x} = f(x, t) + b(t)u \tag{1}$$

where x is the displacement of one of the three axis stages, $f(x, t)$ is a function of the state variables, $b(t)$ is the control gain and $u(t)$ is the control voltage.

The function $f(x, t)$ is an unknown time-varying function with unknown variation bound. However, the bound of the unknown function $b(t)$ can be estimated, i.e., $b_{\min} \leq b(t) \leq b_{\max}$. Define $b(t)$ as

$$b(t) = b_m + \Delta b \tag{2}$$

where b_m is the nominal value and Δb is a bounded uncertainty value.

$$|\Delta b| < \beta, \quad \beta > 0. \tag{3}$$

Here, the functional approximation technique is employed to approximate this unknown function $f(x, t)$ for releasing the model requirements.

3. The controller design

If a piecewise continuous time-varying function $g(t)$ satisfies the Dirichlet conditions, it can be transformed into a generalized Fourier series function expansion within a time interval $[0, T_i]$:

$$g(t) = a_0 + \sum_{n=1}^{\infty} (a_n \cos \omega_n t + b_n \sin \omega_n t) \tag{4}$$

where a_0, a_n and b_n are the Fourier coefficients and $\omega_n = \frac{2n\pi}{T_i}$ is the frequency of the sinusoidal function. Define

$$Z(t) = \begin{bmatrix} 1 & \cos \omega_1 t & \sin \omega_1 t & \cos \omega_2 t & \sin \omega_2 t & \cdots & \cos \omega_n t & \sin \omega_n t \end{bmatrix}^T \tag{5}$$

$$W = \begin{bmatrix} a_0 & a_1 & b_1 & a_2 & b_2 & \cdots & a_n & b_n \end{bmatrix}^T. \tag{6}$$

Then Eq. (4) can be rewritten as

$$g(t) = W^T Z(t) + \varepsilon(t) \tag{7}$$

where $\varepsilon(t)$ is the approximation error. When n is large enough, $g(t)$ can be approximated as

$$g(t) \approx W^T Z(t). \tag{8}$$

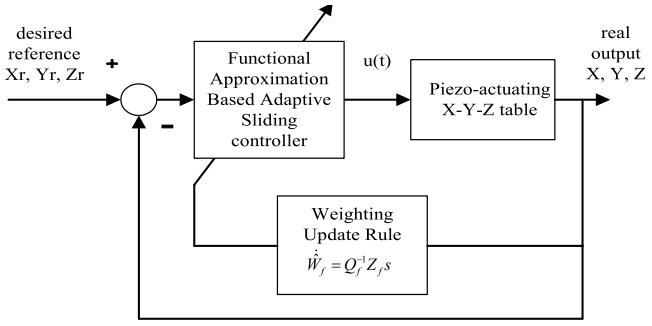

Fig. 3. System control block diagram.

Since the unknown dynamics function $f(x, t)$ in Eq. (1) is a continuous time-varying function, it can be approximated by linear combinations of finite orthogonal basis functions $Z(t)$ to an arbitrarily prescribed accuracy as long as n is large enough:

$$f(x, t) \approx W_f^T Z_f(t) \tag{9}$$

where $Z_f(t)$ is a orthogonal basis function vector and W_f is a weighting coefficient vector. If the number of basis functions is large enough, Eq. (9) can be described as the following approximation form:

$$f(x, t) = W_f^T Z_f(t) \tag{10}$$

where $Z_f(t) = \begin{bmatrix} Z_1(t) & Z_2(t) & \cdots & Z_n(t) \end{bmatrix}^T$, and $W_f = \begin{bmatrix} W_1 & W_2 & \cdots & W_n \end{bmatrix}^T$.

The system control block diagram of this 3D piezoelectrically actuated system is shown in Fig. 3. The sliding surface of the second-order system can be defined as

$$s = \dot{e} + \lambda e \tag{11}$$

where the positive parameter λ implies the convergent rate of x on the sliding surface. The time derivative of s can be derived as

$$\dot{s} = \ddot{e} + \lambda \dot{e} = \ddot{x} - \ddot{x}_r + \lambda \dot{e} \tag{12}$$

where x_r is the desired value of x. Substituting Eq. (1) into (12) yields

$$\dot{s} = f(x, t) + b(t)u - \ddot{x}_r + \lambda \dot{e}. \tag{13}$$

In order to achieve the sliding surface reaching condition and establish the approximation error compensation, the control law $u(t)$ can be designed as

$$u(t) = \frac{1}{b_m}(-\hat{f} + \ddot{x}_r - \lambda \dot{e} - \eta \mathrm{sgn}(s)) \tag{14}$$

where $\hat{f}$ is the functional approximation value of $f(x, t)$.

The positive constant η is a design parameter, for achieving an appropriate robustness. Substituting Eq. (14) into (13) yields

$$\dot{s} = -\eta \mathrm{sgn}(s) + (f - \hat{f}) + \Delta b u. \tag{15}$$

Here, f and $\hat{f}$ can be presented via the functional approximation technique as

$$f = W_f^T Z_f \tag{16}$$

$$\hat{f} = \hat{W}_f^T Z_f \tag{17}$$

where $W_f, \hat{W}_f \in \Re^n$ are weighting vectors and $Z_f \in \Re^n$ is a vector of the basis Fourier series function. Hence, Eq. (15) can be rewritten as

$$\dot{s} = -\eta \mathrm{sgn}(s) + \tilde{W}_f^T Z_f + \Delta b u \tag{18}$$

where $\tilde{W}_f^T = W_f^T - \hat{W}_f^T$. To prove the stability of this control system and find the update laws for vectors $\hat{W}_f$, a Lyapunov function candidate is chosen as

$$V(s, \tilde{W}_f) = \frac{1}{2}s^2 + \frac{1}{2}\tilde{W}_f^T Q_f \tilde{W}_f \tag{19}$$

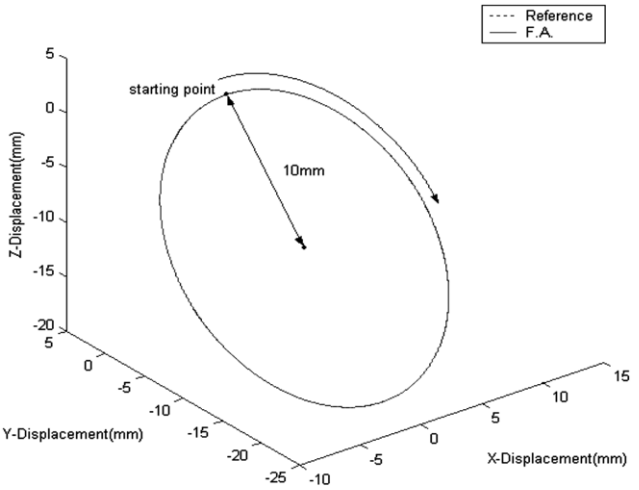

Fig. 4. X–Y–Z table displacement.

where $Q_f \in \Re^{n\times n}$ is a symmetric positive definite matrix. By taking the time derivative of the Lyapunov function candidate, one obtains

$$\dot{V}(s, \tilde{W}_f) = s\dot{s} + \tilde{W}_f^T Q_f \dot{\tilde{W}}_f. \tag{20}$$

Since $\dot{\tilde{W}}_f^T = -\dot{\hat{W}}_f^T$, Eq. (20) can be rewritten as

$$\begin{aligned}\dot{V}(s, \tilde{W}_f) &= s(-\eta \mathrm{sgn}(s) + \tilde{W}_f^T Z_f + \Delta bu) + \tilde{W}_f^T Q_f \dot{\tilde{W}}_f \\ &= -\eta|s| + \tilde{W}_f^T (Z_f s - Q_f \dot{\hat{W}}_f) + \Delta \mathrm{bus}.\end{aligned} \tag{21}$$

The update law for $\hat{W}_f$ is chosen as

$$\dot{\hat{W}}_f = Q_f^{-1} Z_f s. \tag{22}$$

Then, Eq. (21) can be further rewritten as

$$\dot{V} = -\eta|s| + \Delta \mathrm{bus}. \tag{23}$$

In order to cover the uncertainty of the unknown function $b(t)$, and establish an appropriate robustness, the parameter η can be specified as

$$\eta = \beta u_{\max}. \tag{24}$$

Then Eq. (23) yields

$$\dot{V} \leq 0. \tag{25}$$

Eq. (25) means that this control system stability can be guaranteed by using the update laws. On the basis of Barbarlet's lemma [14], the convergence of the system output error can be guaranteed by using the control law $u(t)$, Eq. (14).

4. Experimental results

In order to investigate the control performance of the proposed controller, the following experiments are performed. The sampling frequency is chosen as 1000 Hz. The sliding surface parameter λ is chosen as 700, 900 and 1500 for the X axis, Y axis and Z axis, respectively. The robustness parameter η can be estimated on the basis of Eq. (19). It is selected as 23 000, 29 000 and 30 000 for the X axis, Y axis and Z axis, respectively. In order to improve the control law chattering behavior, the $\mathrm{sgn}(s)$ function in Eq. (9) is replaced by the saturation function $\mathrm{sat}(s/\phi)$ with a boundary layer thickness $\phi = 0.1$ for all the three axes. The weighting matrix Q_f of the Fourier series function coefficients is set as a small constant matrix $Q_f = 0.01[I]$, to increase the convergence speed. 31 terms of Fourier series functions were used for the functional approximation based adaptive sliding controller.

First, an oblique circular contour 2 cm in diameter is designed for the 3D motion tracking control. The experimental result on the tracking response of this 3D system is shown in Fig. 4. The tracking errors for the X, Y and Z axes are shown in Figs. 5–7. It can be observed that the maximum steady-state tracking errors are 0.035 mm, 0.03 mm and 0.03 mm for

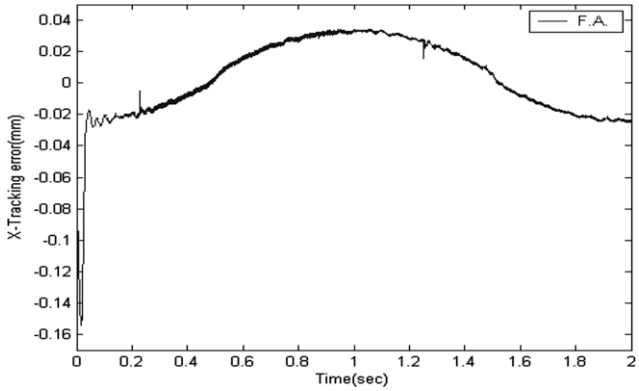

Fig. 5. Tracking error for the X axis.

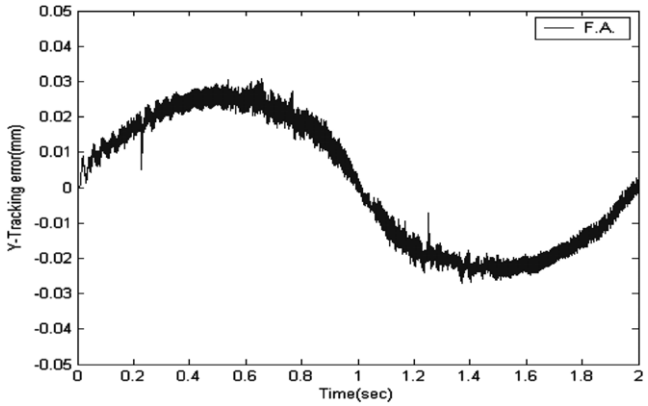

Fig. 6. Tracking error for the Y axis.

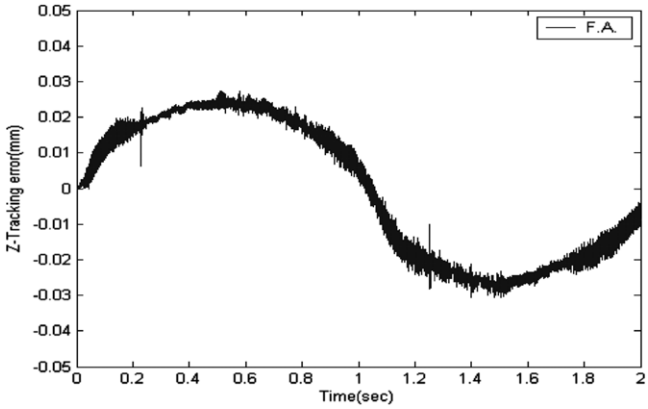

Fig. 7. Tracking error for the Z axis.

the X, Y and Z axes, respectively. The root mean square (RMS) values of the tracking errors are 0.0233 mm, 0.009 mm and 0.010 mm for the X, Y and Z axes, respectively.

Then, a drilling process control using the designed controller is investigated to verify the effectiveness of the proposed controller. A matrix-type drilling of holes with a 0.2 mm diameter trajectory, shown in Fig. 8, is designed for the 3D motion tracking control. The experimental result for the tracking response of this drilling process control is shown in Fig. 9. The tracking responses for the X, Y and Z axes are shown in Figs. 10–12, respectively. The maximum steady-state tracking errors can be controlled as smaller than 0.03 mm for all the three axes. The microscope image of the drilling of holes is shown in Fig. 13. It can be observed that a good control performance can be obtained for a drilling process by using the proposed functional approximation based adaptive sliding controller.

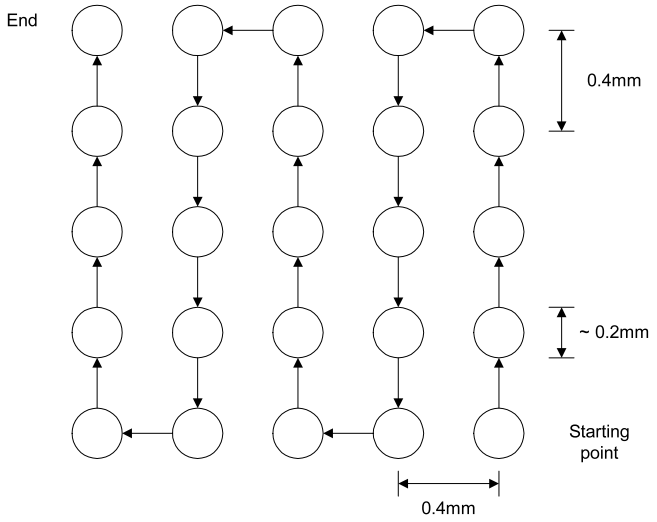

Fig. 8. Matrix-type drilling process trajectory.

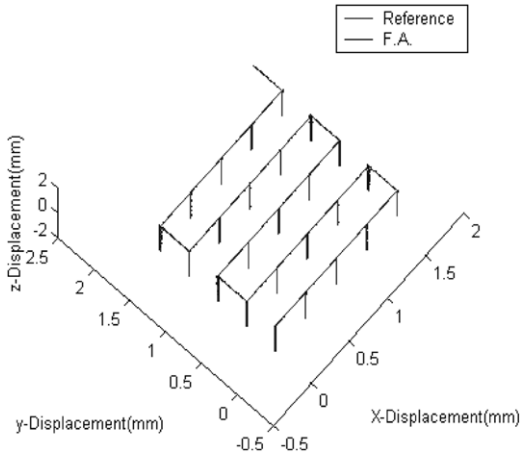

Fig. 9. Tracking response of the drilling process control.

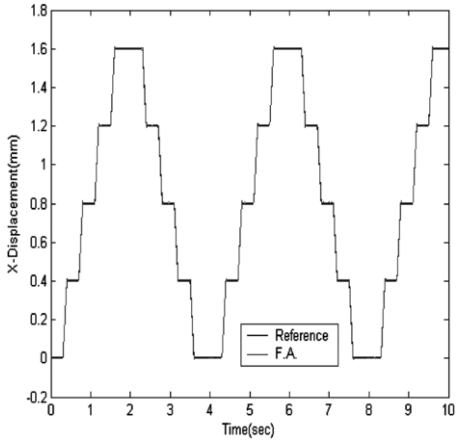

Fig. 10. Tracking response for the *X* axis for the drilling process control.

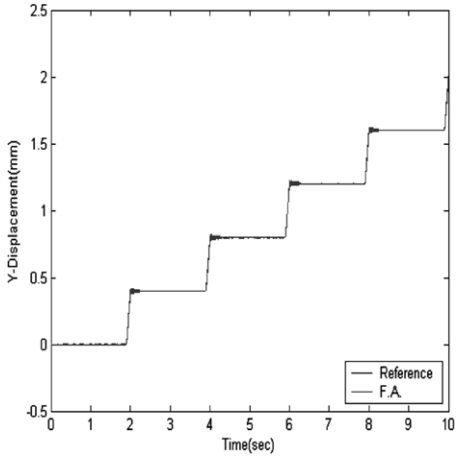

Fig. 11. Tracking response for the Y axis for the drilling process control.

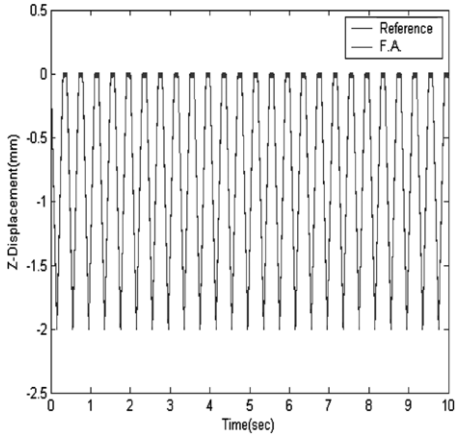

Fig. 12. Tracking response for the Z axis for the drilling process control.

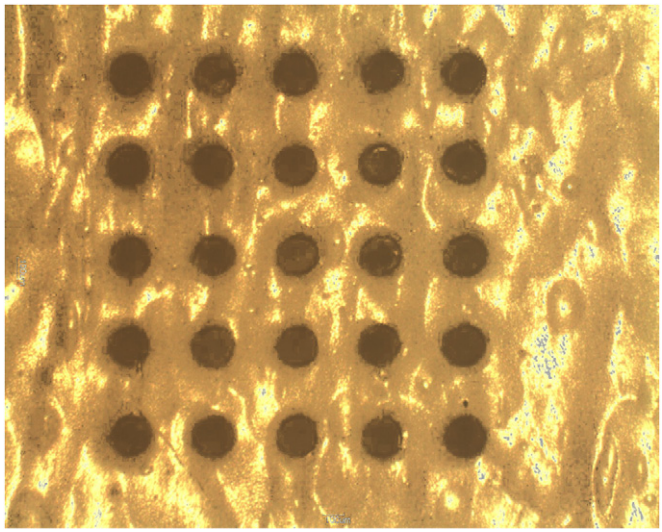

Fig. 13. Microscope image of the drilling of holes.

5. Conclusions

A functional approximation based adaptive sliding controller is developed and successfully employed to control a 3D piezoelectrically actuated system in this paper. In addition, a drilling process control using the designed controller is investigated to verify the effectiveness of the proposed controller. Fourier series functions can be used to approximate the nonlinear time-varying function for designing a sliding-mode controller and achieving good control performance. The steady-state tracking error can be controlled to less than 0.035 mm for all three axes. The proposed approach can be effectively applied to control the 3D piezoelectrically actuated system.

Acknowledgment

The financial support of this research by the National Science Council of the R.O.C. under Grant No. NSC 98-2221-E-131-015 is greatly appreciated.

References

[1] C.J. Lin, S.R. Yang, Precise positioning of piezo-actuated stages using hysteresis-observer based control, Mechatronics 16 (7) (2006) 417–426.
[2] T. Chang, X. Sun, Analysis and control of monolithic piezoelectric nano-actuator, IEEE Trans. Control Syst. Technol. 9 (1) (2001) 69–75.
[3] S. Bashash, N. Jalili, Robust multiple frequency trajectory tracking control of piezoelectrically driven micro/nanopositioning systems, IEEE Trans. Control Syst. Technol. 15 (5) (2007) 867–878.
[4] H.C. Liaw, B. Shirinzadeh, J. Smith, Robust motion tracking control of piezo-driven flexure-based four-bar mechanism for micro–nano manipulation, Mechatronics 18 (2) (2008) 111–120.
[5] G. Song, J. Zhao, X. Zhou, J.Alexis De Abreu-García, Tracking control of a piezoceramic actuator with hysteresis compensation using inverse Preisach model, IEEE/ASME Trans. Mechatronics 10 (2) (2005) 198–209.
[6] T. Meurer, A. Kugi, Tracking control design for a wave equation with dynamic boundary conditions modeling a piezoelectric stack actuator, Int. J. Robust Nonlinear Control 21 (5) (2011) 542–562.
[7] C.J. Lin, P.T. Lin, Tracking control of a biaxial piezo-actuated positioning stage using generalized Duhem model, Comput. Math. Appl. 64 (5) (2012) 766–787.
[8] S.H. Chang, C.K. Tseng, H.C. Chien, An ultra-precision $XY\theta_z$ piezo-micropositioner. Part I: design and analysis, IEEE Trans. Ultrason. Ferroelectr. Freq. Control 46 (4) (1999) 897–905.
[9] R.F. Fung, W.C. Lin, System identification and contour tracking of a plane-type 3-DOF ($XY\theta_z$) precision positioning table, IEEE Trans. Control Syst. Technol. 18 (1) (2010) 22–34.
[10] H.T. Yau, C.C. Wang, C.T. Hsieh, C.C. Cho, Nonlinear analysis and control of the uncertain micro-electro-mechanical system by using a fuzzy sliding mode control design, Comput. Math. Appl. 61 (8) (2011) 1912–1916.
[11] D.Y. Chen, W.L. Zhao, X.Y. Ma, R.F. Zhang, No-chattering sliding mode control chaos in Hindmarsh–Rose neurons with uncertain parameters, Comput. Math. Appl. 61 (10) (2011) 3161–3171.
[12] C.L. Kuo, Design of a fuzzy sliding-mode synchronization controller for two different chaos systems, Comput. Math. Appl. 61 (8) (2011) 2090–2095.
[13] H.Y. Chen, S.J. Huang, A new model-free adaptive sliding controller for active suspension system, Internat. J. Systems Sci. 39 (1) (2008) 57–69.
[14] K.S. Narendra, A.M. Annaswamy, Stable Adaptive Systems, Prentice Hall, Englewood Cliffs, 1989.